

Real-time Video Imaging of Mechanical Motions of a Single Molecular Shuttle

Toshiki Shimizu,[†] Dominik Lungerich,[†] Joshua Stuckner,[‡] Mitsuhiro Murayama,^{‡,§,||} Koji Harano^{*,†}, Eiichi Nakamura^{*,†}

[†]*Department of Chemistry, The University of Tokyo, 7-3-1 Hongo, Bunkyo-ku, Tokyo 113-0033, Japan*

[‡]*Materials Science and Engineering Department, Virginia Tech, Blacksburg, VA 24061, USA*

[§]*Reactor Materials and Mechanical Design Group, Energy and Environmental Directorate, Pacific Northwest National Laboratory, Richland, WA 99352*

^{||}*Institute for Materials Chemistry and Engineering, Kyushu University, Kasuga, Fukuoka 816-8580, Japan*

Supporting Information Placeholder

ABSTRACT: Miniatured machines has open up a new dimension of chemistry, studied usually as an average over numerous molecules or for a single molecule bound on a robust substrate. Mechanical motions at a single molecule level, however, are under quantum control, strongly coupled with fluctuations of its environment -- a system rarely addressed because an efficient way of observing the nanomechanical motions in real time is lacking. Here, we report sub-ms sub-Å precision in situ video imaging of a single fullerene molecule shuttling, rotating, and interacting with a vibrating carbon nanotube, using an electron microscope, a fast camera, and a denoising algorithm. We have realized high spatial precision of distance measurement with the standard error of the mean as small as ± 0.01 nm, and revealed the rich molecular dynamics, where motions are non-linear, stochastic and often non-repeatable, and a work and energy relationship at a molecular level previously undetected by time-averaged measurements or microscopy.

Single-molecule mechanics of miniature molecular machines¹ is an unexplored field of chemistry.² At such a minute scale as molecules in a carbon nanotube (CNT)^{3,4} the molecule becomes strongly interacting with its fluctuating environment, rendering the mechanics non-linear, stochastic, and even non-repeatable—a system difficult to address because an efficient way of observing the nanomechanical molecular motions in real time is lacking. Here, we report in situ video imaging of single molecules shuttling, rotating, and interacting with a mechanically vibrating CNT illustrated for a shuttling C₆₀ dimer (cartoon in Figure 1a and simulation in Figure 1b), using an aberration-corrected electron microscope, a direct electron detection (DED) camera, and Chambolle total variation (CTV) denoising.⁵ With this setup of molecular electron

microscopy, we were able to record strongly correlated motions of the CNT that vibrates stochastically a few times per second, and the molecule that translates stochastically within 1.875 ms. This molecular shuttling represents a prototypal single-molecular machine⁶ – a particle in a box where a particle has a finite mass having a potential shown in Figure 1c.⁷ Stochastic translational motion of C₆₀ dimers in CNT was previously proposed to be a non-thermal event,⁸ which is supported by the temperature insensitivity of the frequency of the events observed in this study. The video images with sub-ms sub-Å precision reported below now reveal the rich dynamics, where a kinetic energy is recurrently supplied from the mechanically vibrating CNT⁹ to the molecule, and the CNT was deformed by the translating molecule – a work and energy relationship at a molecular level previously undetected by time-averaged measurements or microscopy. The technique opens a new dimension in the study of non-linear mechanics of a single molecule¹⁰ at hitherto unavailable spatio-temporal precision, expected to be useful for studies of conformational change and reactions at single molecule level.

The shuttling motion occurring in a weakly chaotic manner,¹¹ one cannot use the conventional fast imaging method, pump-probe microscopy¹² which requires the events observed to be repeatable and easily reproducible.^{13,14} This limitation would be lifted by fast electron microscopy (EM) imaging,¹⁵ which has not been achieved for a variety of reasons.^{16,17} For example, a 78-ms video image (Figure 1b) illustrates translation and rotation motions of a C₆₀ dimer (6–7, colored in light blue),^{18,19} the structure of which was previously discussed computationally²⁰ and experimentally.²¹ The factors that limit the potential of EM include low image contrast due to the small cross-section of light elements, lack of spatial periodicity of the molecular specimens, and

characteristics of EM and detector (aberration, spatial and pixel resolution, frame rate, signal and noise intensity).^{22, 23} An ultrafast camera alone does not solve the problems because the high frame rate proportionately reduces the electron dose per frame, making a single-frame image practically invisible. The present CTV denoising strategy coupled with a fast DED camera has achieved a time resolution of 0.9 ms and a localization precision of 0.01 nm for imaging of non-periodic molecular structures. A 2.5-ms time resolution has so far been the fastest EM time resolution recorded for imaging of crystal facet development.¹⁵ The demonstrated utility of EM for single molecule dynamics,¹⁴ combined with recent reports on micro electron diffraction of small organic molecules,^{24,25,26} will encourage more frequent use of EM in chemical research.

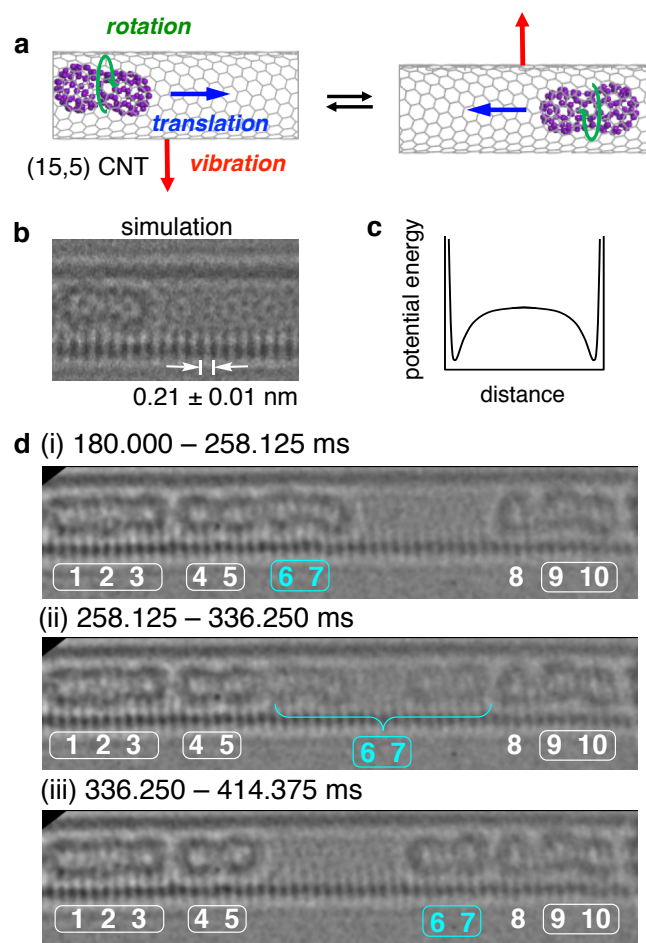


Figure 1. Motions of fullerene molecules in CNT. (a) A rigid body model showing motions of a kidney-shaped C₆₀ dimer in a chiral CNT. (b) A simulation image of (15,5)CNT and a kidney-shaped C₆₀ dimer reported by Osawa and Tománek as compound 14.²⁰ The vertical pitches with 0.21 nm periodicity on the CNT walls are derived from the graphitic lattice. (see SI for EM image simulation). (c) A schematic potential energy of a molecule in a void space of CNT based a reported computational data.⁷ (d) Three video frames with an exposure time of 78.125 ms/frame (12.8 fps) at 298 K, showing C₆₀ dimer translation in frame ii. The acceleration

voltage was 80 kV with an electron dose rate of $2.7 \times 10^6 \text{ e}^- \text{ nm}^{-2} \text{ s}^{-1}$. The vertical pitch with 0.21 nm periodicity on the CNT walls fits with a model based on (15,5) CNT (Figure 1b, d; see Supporting Information for details). In the video images in Figures 1b, 2e and 3, the frame is referenced to an arbitrary time zero, which, in this case, is 6 s after the start of the observation. The translation took place quickly in less than 1.875 ms at 300.000 ms as will be illustrated in Figure 3. Scale bar, 1 nm throughout this work.

Our first goal was to obtain molecular images from an ultrafast camera that outputs 1600 fps or 0.625 ms/frame; $0.021 \text{ nm} \times 0.021 \text{ nm pixel}^{-1}$ at 400 k magnification). The signal-to-noise ratio (SNR) being as low as 0.05, a single frame hardly reveals any molecules or CNT (Figure 2a; see the original video in Video S1). At this frame rate, one pixel receives only 0.83 electrons/frame (or $1,875 \text{ e}^- \text{ nm}^{-2}$) at the maximum detector-safe electron dose rate (EDR) of $3 \times 10^6 \text{ e}^- \text{ nm}^{-2} \text{ s}^{-1}$. It is only after superimposing 50 frames (31.25 ms/frame) by a pixel averaging method that the molecular images become clear enough (Figure 2b; SNR = 0.20). The molecules on the left have a van der Waals (vdW) contact (intermolecular distance $d = 1.01 \text{ nm}$), while those in the center are a [2 + 2] dimer ($d = 0.90 \text{ nm}$, Figure 2c).¹³ With the superimposition, however, we lose the advantage of the 1600-fps camera because the SNR gain is proportional to the square root of the exposure time, to which the time resolution is inversely proportional.

We cannot rely on contrast enhancement methods²⁷ for imaging of moving objects, and instead explored image processing methods of the raw EM images.^{28, 29} After a comparison of several methods, we found that CTV⁵ denoising and superposition exhibit a good balance between noise reduction and preservation of original signals; in particular, edge information essential for molecular imaging. Thus, we obtain a 0.625-ms/frame image with SNR = 0.15 where we identify the molecules (Figure 2c). After simultaneous three-frame CTV superposition and denoising (1.875 ms/frame, Figure 2d), we see the molecules very clearly with SNR = 0.30. With denoising, we can thus achieve a comparable SNR at a 17 times faster frame rate (Figure 2b vs. 2d).

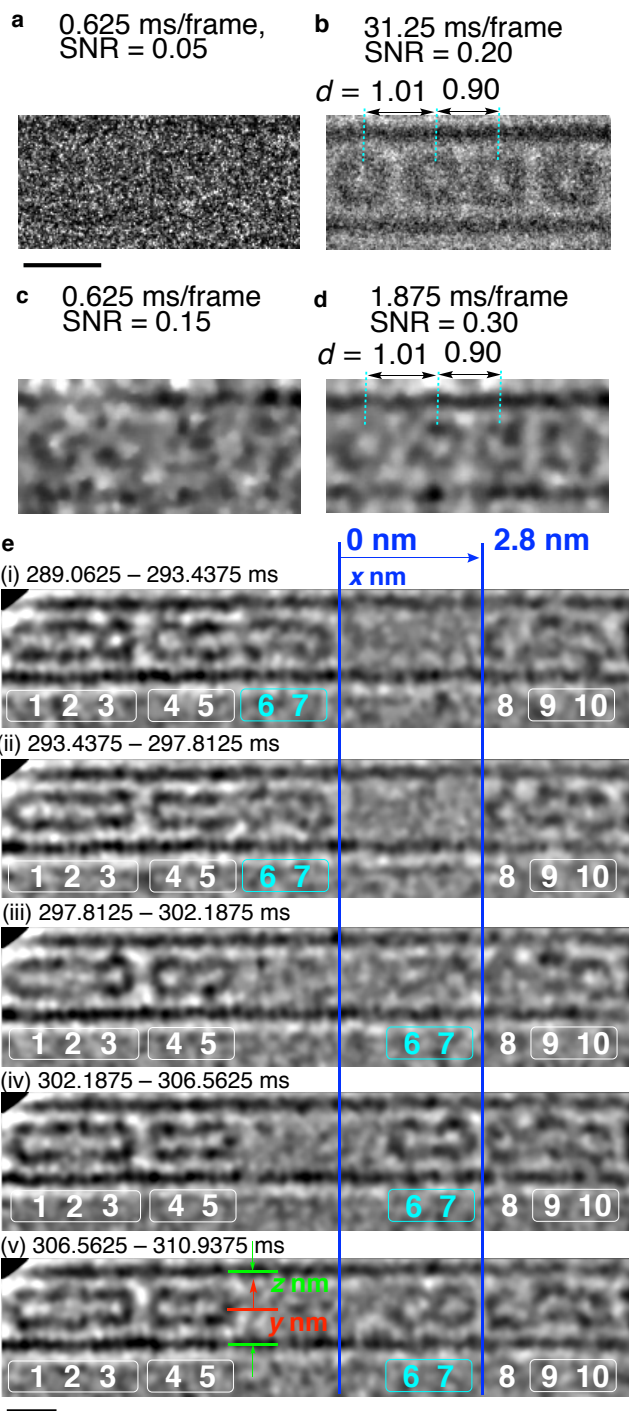


Figure 2. Fast video imaging of fullerene molecules with CTV denoising and superimposition. An underfocus of 12 ± 2 nm was used to maintain stable imaging of the molecules throughout this study. The same time scale as in Fig. 1d. (a) A single-frame original image of C_{60} molecules at 423 K taken at 0.625 ms/frame with a DED camera at 80 kV and an EDR of $1.3 \times 10^6 e^- nm^{-2} s^{-1}$. (b) Fifty-frame superimposition without denoising. Distance d shown in nm. (c) CTV denoised single-frame image of the molecule shown in (a). (d) Three-frame superimposition of (c) (1.875 ms exposure). (e) Motions of a C_{60} dimer in a vibrating CNT (80 kV, EDR = $2.7 \times 10^6 e^- nm^{-2} s^{-1}$). The same video as Figure 1b at 298 K but reanalyzed at 4.375 ms/frame. The x , y , and z values

are defined as shown. See also the Supporting information for larger images (Figure S7) and the video (Video S2).

With the effective denoising protocol in hand, we next examined the ‘pebble-in-a-maraca’ translation motions of fullerene molecules in a vibrating CNT. Through observation of roughly 400 molecules in CNTs for a total observation time of 10 min over roughly a million frames at 0.625 ms/frame (roughly 380 million images of C_{60} in total), we found a few tens of cases of translation taking place within 1.875 ms, out of which four events seen on two molecules were suitable precise analysis (Figures 2e, 3, and 4). Other events suffered either excessive CNT vibration or overlapping with neighboring CNTs. Figure 2e illustrates the same molecular events as the one in Figure 1b, but at 18 times faster frame rate of 4.375 ms/frame, revealing that the dimer (6–7) translated in the 297.8125–302.1875 ms frame where we see a faint image of the dimer (colored in light blue: see Video S2 for the original video images). Here, we observed molecular translation and rotation, as well as CNT vibration and deformation, which we quantify with parameters x (translation of the molecule from origin), y (a parameter represents the lateral CNT vibration; displacement of the center of CNT from the place at time zero), and z (CNT diameter) in nm (For details on these parameters, see Supporting Information).

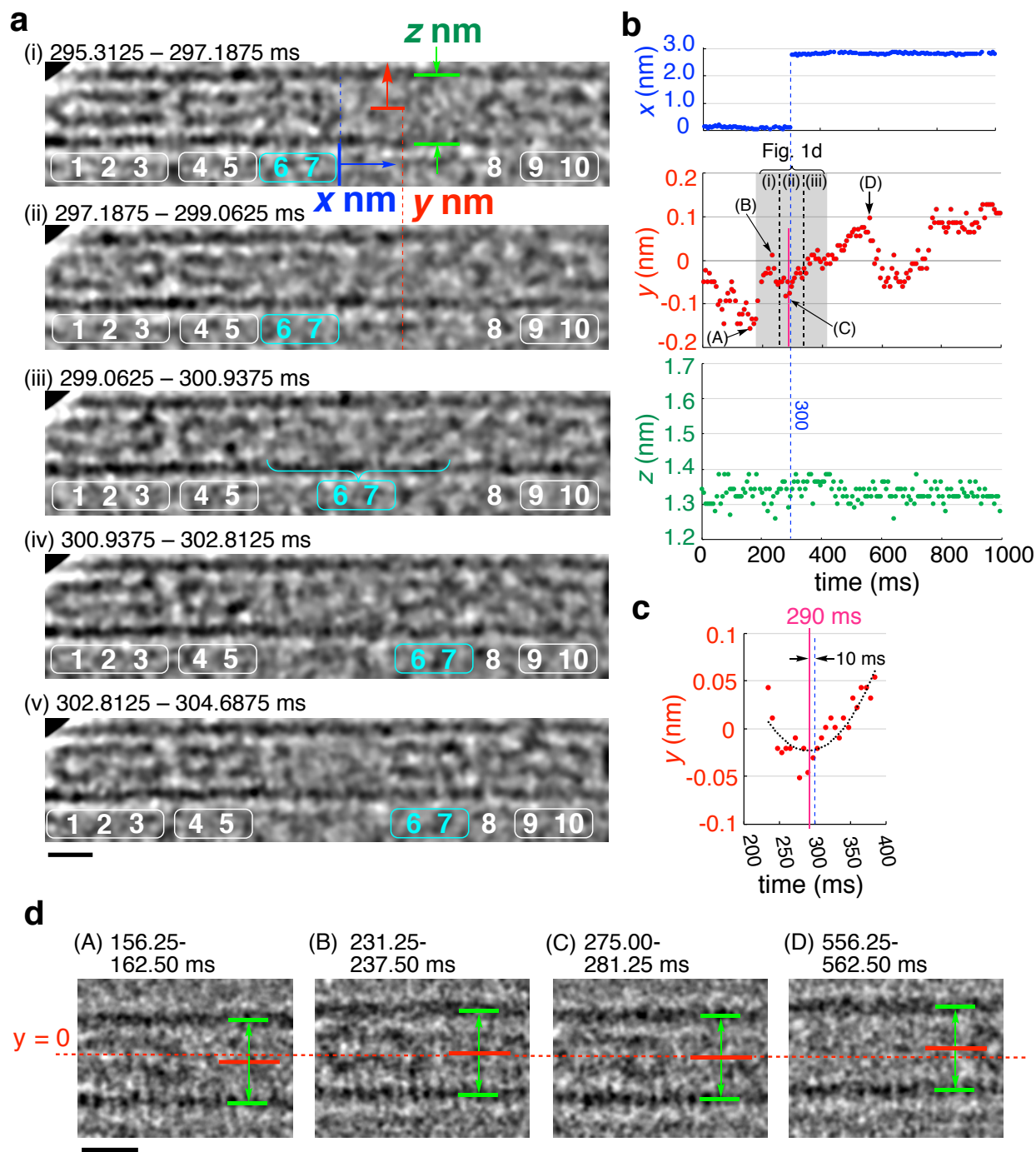


Figure 3. SMART-EM video frames showing the motions of a C_{60} dimer in a vibrating CNT. (a) The same dimer translation as Figure 1b at 298 K, but reanalyzed at 1.875 ms/frame. The x , y , and z values are plotted against time in Figure 2b. See the Supporting Information (Video S2) (80 kV, EDR = $2.7 \times 10^6 \text{ e}^- \text{ nm}^{-2} \text{ s}^{-1}$). (b) Oligomer translation (blue), CNT vibration (red), and deformation (green) taken every 6.25 ms. The time frames highlighted in gray corresponds to time frames of Figure 1b (i)-(iii). (c) Expansion of 290 ms area of CNT vibration with quadratic function curve fitting, dimer translation (blue dashed), and maximum point of vibration (pink). (d) Four representative frames (A)-(D) in Figure 3b (6.25 ms/frame) illustrating the vibration of the CNT. Red bar indicates the center of CNT (y) calculated from the two edges of CNT (green).

At a faster frame rate of 1.875 ms/frame in Figure 3a, we found that translation and rotation of the dimer (6–7) are strongly correlated to CNT vibration and deformation. In a sequence of frames ii to iv in Figure 3a, the dimer translated between 299.0625 and 300.9375 ms (300 ms \pm 0.9375 ms, colored in light blue) until it hit molecule 8.

Figure 3b quantitatively summarizes the dimer motion (x) in blue, together with the CNT vibration (y) taking place roughly 10 times during 1000 ms with an amplitude of 0.1 nm or less. Here, we find that one of the vibration events caused a single translation event. The CNT diameter (green) changed by less than ± 0.05 nm. As magnified in

Figure 3c, we see that the translation (blue dashed line) took place 10 ms after the CNT vibration at its maximum amplitude at 290 ms (pink solid line). Here, the dimer received enough kinetic energy to break the vdW contact with its neighbor 4–5 (estimated to be ca. 0.3 eV; cf. Figure 1c).³⁰ The dimer 6–7 rotated during the translation (cf. Figure 1b, i vs. iii). Thus, the rightward translation took place when the CNT was changing its direction of vibration from a negative to a positive direction, (Figure 3b, red and blue), and longitudinal rotation also took place.

(in blue dashed lines) took place within 11–40 ms of the time of maximum displacement of the CNT vibration (pink). Thus, two rightward translation events took place when the CNT was changing its direction of vibration from a positive to a negative lateral direction (Figure 4c, and 4e), and one leftward translation event (Figure 4d) took place upon change from a negative to a positive direction. Because of the irregular shape of the oligomer, the translation resulted in an expansion of the CNT by as much as 19% during the 1.8-s observation time (Figure 4b in green), indicating that the kinetic energy given to

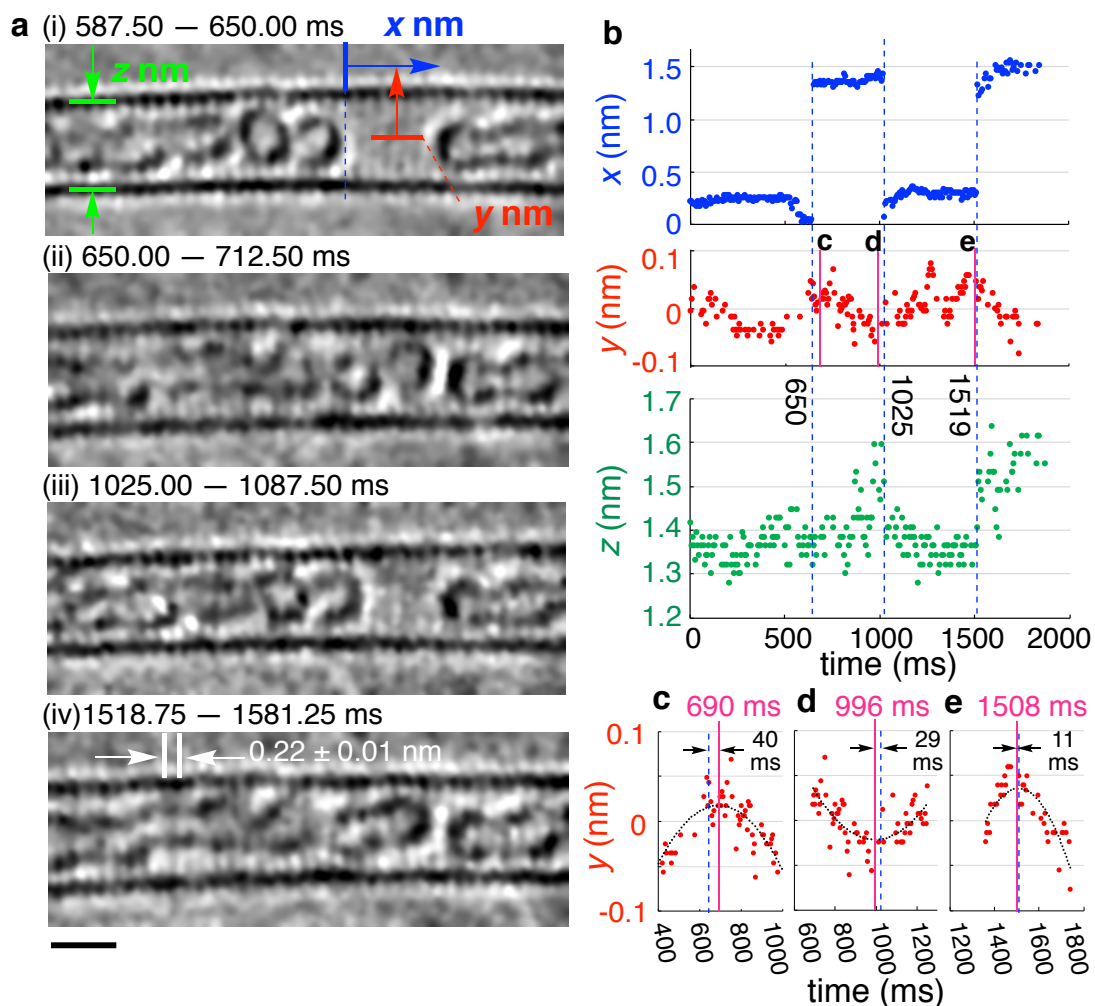


Figure 4. SMART-EM video frames showing the motions of a C_{60} oligomer in a vibrating CNT (80 kV, EDR = 4.3×10^6 $e^- \text{ nm}^{-2} \text{ s}^{-1}$). (a) Oligomer translation at 298 K. See also the Supporting information for larger images (Figure S8-10) and the video (Video S3). The time zero is set to be 9 s after the start of the observation. (b) The x , y , and z values are plotted against time. (c–e) Expansion of 690, 996, and 1508 ms areas of vibration with quadratic function curve fitting, oligomer translation (blue dotted), and maximum point of vibration (pink).

Figure 4a provides further evidence on the coupling of molecular translation and rotation to with vibration of the CNT. Here, an oligomer on the left, made of at least seven C_{60} molecules, shuttled back and forth three times unidirectionally each time accompanying molecular rotation, and each of the three translation events was triggered by a single CNT vibration (compare Figure 3b in blue and red). Figures 4c, d, and e show that all translation events

the oligomer from the CNT vibration was large enough to deform the CNT – a work and energy relationship at a molecular level previously undetected by time-averaged measurements and microscopy. Note that translation of the dimer (at 300 ms, Figure 3b) and of the oligomer (at 650 ms, Figure 4b) took place without change of the CNT diameter z , suggesting the deformation seen at 1025 and

1519 ms in Figure 4b is the result of the translation and not vice versa.

The experimental data obtained by molecular electron microscopy provide several implications on the mechanics of the semi-chaotic molecular shuttling. First, the CNT vibration event seen real time at a ms and sub-Å level took place stochastically, roughly 10 times per second – a frequency suggestive of mechanical motion instead of thermal vibration.⁹ Second, the translation events are synchronized to the CNT vibration, taking place stochastically a few to several times per minute at both 298 K and 423 K. This temperature insensitivity of the frequency of the translation stands in sharp contrast to the temperature-dependence of the reaction rate of the C₆₀ dimerization reaction.¹³ Third, each translation event took place only when the CNT vibrated at its maximum amplitude, while many other vibrational events did not cause translation, indicating that neither direct electron bombardment of the fullerene molecule nor CNT deformation (see above) is not the cause of the translation. Fourth, all translation events accompanied longitudinal molecular rotation (direction of the rotation unknown at this time). Fifth, molecular translation resulted in deformation of the CNT. Lastly but most notably, the correlation between the direction of CNT vibration and that of molecular translation, coupled with rotation poses an intriguing question on how lateral vibration of CNT can induce the axial translation and longitudinal rotation of the molecule, where the helical hexagon array of the graphitic wall may play a role.³¹

In summary, we found that the molecule and the CNT container as a whole behave as a mechanical coupled oscillator, where the molecule motion is coupled with the mechanical motion of the CNT container, providing an answer to our long standing question why the molecules attached to a CNT moves so infrequently and stochastically. A corollary to the present structural analysis is high spatial precision of molecular distances measured by fast SMART-EM imaging. From a 100-distance data set on [x](#)

in Figure 3b (after time 300 ms), we obtained $x = 2.79$ nm with a standard error of 0.003 nm with a confidence level of 68%, and $x = 2.79 \pm 0.01$ nm with a confidence level of 99%. Furthermore, the average distance d determined for 30 superimposed images for the vdW contact between two C₆₀ molecules at 423 K (cf. Figure 2d) was 1.00 ± 0.01 nm with a confidence level of 99%, agreeing with the X-ray crystallographic data of 1.002 ± 0.001 nm at 300 K.³²

ASSOCIATED CONTENT

Supporting Information. Experimental procedure, additional microscopic images, and video captions are available free of charge via the Internet at <http://pubs.acs.org>.

AUTHOR INFORMATION

Corresponding Author

harano@chem.s.u-tokyo.ac.jp

nakamura@chem.s.u-tokyo.ac.jp

ACKNOWLEDGMENT

We thank N. Mamizu and H. Furukawa (SYSTEM IN FRONTIER INC.) for the automated cross-correlation image analysis. This research is supported by MEXT (KAKENHI 19H05459), Japan Science and Technology Agency (SENTAN JPMJSN16B1) and the National Science Foundation (EAPSI #1713989 and DMREF #1533969). J.S. and M.M. acknowledge the Virginia Tech National Center for Earth and Environmental Nanotechnology Infrastructure (NanoEarth) (NSF ECCS #1542100). T.S. acknowledges financial support from the ALPS program (MEXT). D.L. acknowledges the financial support as an international research fellow from the Japan Society for the Promotion of Science (JSPS) and the Alexander von Humboldt Foundation.

REFERENCES

- (1) Erbas-Cakmak, S.; Leigh, D. A.; McTernan, C. T.; Nussbaumer, A. L. Artificial molecular machines. *Chem. Rev.* **2015**, *115*, 10081–10206.
- (2) Kudernac, T.; Ruangsapichat, N.; Parschau, M.; Maciá, B.; Katsonis, N.; Harutyunyan, R. S.; Ernst, K.; Feringa, B. L. Electrically driven directional motion of a four-wheeled molecule on a metal surface. *Nature* **2011**, *479*, 208–211.
- (3) Warner, J. H.; Ito, Y.; Zaka, M.; Ge, L.; Akachi, T.; Okimoto, H.; Porfyraakis, K.; Watt, A. A. R.; Shinohara, H.; Briggs, G. A. D. Rotating fullerene chains in carbon nanopeapods. *Nano. Lett.* **2008**, *8*, 2328–2335.
- (4) Su, H.; Goddard III, W. A.; Zhao, Y. Dynamic friction force in a carbon peapod oscillator. *Nanotechnology* **2006**, *17*, 5691.
- (5) Chambolle, A. An algorithm for total variation minimization and applications. *J. Math. Imaging Vis.* **2004**, *20*, 89–97.
- (6) Anelli, P. L.; Spencer, N.; Stoddart, J. F. A molecular shuttle. *J. Am. Chem. Soc.* **1991**, *113*, 5131–5133.
- (7) Kang, J. W.; Hwang, H. J. Fullerene shuttle memory device: Classical molecular dynamics study. *J. Phys. Soc. Jpn.* **2004**, *73*, 1077–1081.
- (8) Smith, B. W.; Monthieux, M.; Luzzi, D. E. *Chem. Phys. Lett.* **1999**, *315*, 31–36.
- (9) Barnard, A. W.; Zhang, M.; Wiederhecker, G. S.; Lipson, M. & McEuen, P. L. Real-time vibrations of a carbon nanotube. *Nature* **2019**, *566*, 89–93.
- (10) Sotomayor, M.; Schulten, K. Single-molecule experiments in vitro and in silico. *Science* **2007**, *316*, 1144–1148.
- (11) Poot, M.; van der Zant, H. S. J. Mechanical systems in the quantum regime. *Phys. Rep.* **2012**, *511*, 273–336.
- (12) Zewail, A. H. Four-dimensional electron microscopy. *Science* **2010**, *328*, 187–193.
- (13) Okada, S.; Kowashi, S.; Schweighauser, L.; Yamanouchi, K.; Harano, K.; Nakamura, E. Direct microscopic analysis of individual C₆₀ dimerization events: kinetics and mechanisms. *J. Am. Chem. Soc.* **2017**, *139*, 18281–18287.
- (14) Nakamura, E.; Harano, K. Chemical kinetics study through observation of individual reaction events with atomic-resolution electron microscopy. *Proc. Jpn. Acad., Ser. B.* **2018**, *94*, 428–440.
- (15) Liao, H.-G.; Zhrebetsky, D.; Xin, H.; Czarnik, C.; Ercius, P.; Elmlund, H.; Pan, M.; Wang, L.-W.; Zheng, H. Facet development during platinum nanocube growth. *Science* **2014**, *345*, 916–919.
- (16) Koshino, M.; Tanaka, T.; Solin, N.; Suenaga, H.; Isobe, H.; Nakamura, E. Imaging of single organic molecules in motion. *Science* **2007**, *316*, 853.

- (17) Skowron, S. T.; Chamberlain, T. W.; Biskupek, J.; Kaiser, U.; Besley, E. Chemical reactions of molecules promoted and simultaneously imaged by the electron beam in transmission electron microscopy. *Acc. Chem. Res.* **2017**, *50*, 1797–1807.
- (18) Smith, B. W.; Monthieux, M.; Luzzi, D. E. Encapsulated C₆₀ in carbon nanotubes. *Nature* **1998**, *396*, 323–324.
- (19) Khlobystov, A. N.; Britz, D. A.; Briggs, G. A. D. Molecules in carbon nanotubes. *Acc. Chem. Res.* **2005**, *38*, 901–909.
- (20) Han, S.; Yoon, M.; Berber, S.; Park, N.; Osawa, E.; Ihm, J.; Tománek, D. Microscopic mechanism of fullerene fusion. *Phys. Rev. B* **2004**, *70*, 113402.
- (21) Koshino, M.; Niimi, Y.; Nakamura, E.; Kataura, H.; Okazaki, T.; Suenaga, K.; Iijima, S. Analysis of the reactivity and selectivity of fullerene dimerization reactions at the atomic level. *Nat. Chem.* **2010**, *2*, 117–124.
- (22) Williams, D. B.; Carter, C. B. *Transmission Electron Microscopy*; Springer: New York, 2009.
- (23) Jiang, Y.; Chen, Z.; Han, Y.; Deb, P.; Gao, H.; Xie, S.; Purohit, P.; Tate, M. W.; Park, J.; Gruner, S. M.; Elser, V.; Müller, D. A. Electron ptychography of 2D materials to deep sub-ångström resolution. *Nature* **2018**, *559*, 343–349.
- (24) van Genderen, E.; Clabbers, M. T. B.; Das, P. P.; Stewart, A.; Nederlof, I.; Barentsen, K. C.; Portillo, Q.; Pannu, N. S.; Nicolopoulos, S.; Gruene, T.; Abrahams, J. P. Ab initio structure determination of nanocrystals of organic pharmaceutical compounds by electron diffraction at room temperature using a Timepix quantum area direct electron detector. *Acta Cryst.* **2016**, *A72*, 236–242.
- (25) Gruene, T.; Wennmacher, J. T. C.; Zaubitzer, C.; Holstein, J. J.; Heidler, J.; Fecteau-Lefebvre, A.; De Carlo, S.; Müller, E.; Goldie, K. N.; Regeni, I.; Li, T.; Santiso-Quinones, G.; Steinfeld, G.; Handschin, S.; van Genderen, E.; van Bokhoven, J. A.; Clever, G. H.; Pantelic, R. Rapid Structure Determination of microcrystalline molecular compounds using electron diffraction. *Angew. Chem. Int. Ed.* **2018**, *57*, 16313–16317.
- (26) Jones, C. G.; Martynowycz, M. W.; Hattne, J.; Fulton, T. J.; Stoltz, B. M.; Rodriguez, J. A.; Nelson, H. M.; Gonen, T. The cryoEM method microED as a powerful tool for small molecule structure determination. *ACS Cent. Sci.* **2018**, *4*, 1587–1592.
- (27) Zhu, Y.; Ciston, J.; Zheng, B.; Miao, X.; Czarnik, C.; Pan, Y.; Sougrat, R.; Lai, Z.; Hsiung, C. E.; Yao, K.; Pinnau, I.; Pan, M.; Han, Y. Unravelling surface and interfacial structures of a metal-organic framework by transmission electron microscopy. *Nat. Mater.* **2017**, *16*, 532–536.
- (28) Kushwaha, H. S.; Tanwar, S.; Rathore, K. S.; Srivastava, S. Denoising filters for TEM (transmission electron microscopy) image of nanomaterials. *2012 Second International Conference on Advanced Computing & Communication Technologies* **2012**, 276–281.
- (29) Ede, J. M.; Beanland, R. Improving electron micrograph signal-to-noise with an atrous convolutional encoder-decoder. *Ultramicroscopy* **2019**, *202*, 18–25.
- (30) Ginard, C.; Lambin, P.; Dereux, A.; Lucas, A. A. Van der Waals attraction between two C₆₀ fullerene molecules and physical adsorption of C₆₀ on graphite and other substrates. *Phys. Rev. B.* **1994**, *49*, 11425–11432.
- (31) Neek-Amal, M.; Abedpour, N.; Rasuli, S. N.; Naji, A.; Ejtehadi, M. R. Diffusive motion of C₆₀ on a graphene sheet. *Phys. Rev. E* **2010**, *82*, 051605.
- (32) Heiney, P. A.; Fischer, J. E.; McGhie, A. R.; Romanow, A. M.; Denenstien, A. M.; McCauley, J. P. Jr.; Smith, A. P.; Cox, D. E. Oriental ordering transition in solid C₆₀. *Phys. Rev. Lett.* **1991**, *66*, 2911–2914.

Real-time Video Imaging of
a Single Molecular Shuttle

